

THE MEASUREMENT OF AEROSOL OPTICAL THICKNESS IN MINA DURING THE HAJJ SEASON 1426H

S. A. Hashim[#], Sultan Al Sultan^{*}, M. Z. MatJafri[#], K. Abdullah[#] and N. M. Salleh[#]

[#]School of Physics, Universiti Sains Malaysia, 11800 Minden, Penang, Malaysia.
Tel : +604-6533888, Fax : +604-6579150, E-mail : syahamin@yahoo.com , mjafr@usm.my, khirudd@usm.my

^{*}Al Sultan Environmental Research Center. Al Madina Rd., P.O.Box. 242 Riyadh Al Khabra, Al Qassim, Saudi Arabia. Tel: +966504890977, Fax: +96663340366, E-mail: allsultan7@hotmail.com

Commission VII, Working Group VII/8

KEY WORDS: AOT, PM10, Hajj Season, Kriging, Beer-Lambert Law, Spectroradiometer

ABSTRACT:

The aerosol optical thickness (AOT) product can be used to provide an estimate of air quality over the land surface. The measurements have been acquired around Mina, Saudi Arabia during the Hajj season 1426H. A technique based on spectroradiometer measured transmittance data was applied to derive the aerosol optical thickness (AOT) in the atmosphere. We selected the spectral values at 550nm for the present analysis. The PM10 (particles measuring 10-micron or less) were measured simultaneously with the measurements of the transmittance data. An AOT map was generated using Kriging interpolation method. The well known Beer-Lambert law was used in this study to retrieve AOT values from the measured transmittance values. The results show that the AOT values were linearly correlated with the PM10 readings using the spectroradiometer over the land surface in Mina, Saudi Arabia.

1. INTRODUCTION

Satellite remote sensing data sets are widely used to map the geographical distribution of aerosols at high spatial and temporal resolutions and to explore the bulk effects of atmospheric aerosols on the earth's radiation budget. Dust aerosols, which are prevalent over the desert, can be transported to downwind areas thousands of kilometers away from source regions, degrading visibility and air quality, perturbing the radiative transfer in the atmosphere, providing a vector for disease causing organisms, and exacerbating symptoms in people with asthma [Prospero, 1999].

Most of the studies have used aerosol optical thickness to study urban air pollution. Aerosols fall into two main fractions, a coarse 10 micron (PM10) and finer 2.5 micron fraction. The smaller fraction easily penetrates lung tissue and is suspected of causing asthma and related conditions [J. Wang, et al., 2005].

Anthropogenic and natural aerosols are recognized as significant atmospheric substances for the present and future climate changes. They have two effects on the earth's radiation budget. One is a direct effect in which aerosol particles scatter and absorb the solar and thermal radiation. The other is an indirect effect in which they change the particle size and lifetime of cloud droplets acting as cloud condensation nuclei, leading to a cloud albedo change (Takemura, et al., 2002).

In this study, satellite scene from Landsat TM was used for air quality mapping around Mina, Saudi Arabia during the Hajj Season 1426H. The in-situ measurements of atmospheric transmittance values were collected using a handheld spectroradiometer and the AOT values were retrieved from them. A multispectral algorithm was developed based on the atmospheric aerosol characteristic for the estimation of the AOT concentration over desert of Mina, Saudi Arabia. Various algorithms were also tested and the values of their correlation coefficients (R) and root-mean-square deviations (RMS) were

compared. The proposed algorithm was used to generate the AOT map. Finally, the digital image was geometrically corrected to produce an AOT map.

2. STUDY AREA

The selected study area was an urban-desert area of Mina, Saudi Arabia. Figure 1 shows the study area of the Mina, Saudi Arabia. The corresponding PM10 measurements were collected using the DustTrakTM meter at the several selected locations.



Figure 1. The location of the study area

3. ALGORITHM MODEL

An algorithm was developed for AOT determination. The independent variables are the TM visible wavelengths reflectance and thermal infrared band signals.

The atmospheric reflectance due to molecule, R_r , is given by (Liu, et al., 1996)

$$R_r = \frac{\tau_r P_r(\Theta)}{4\mu_s \mu_v} \quad (2)$$

where

τ_r = Aerosol optical thickness (Molecule)

$P_r(\Theta)$ = Rayleigh scattering phase function

μ_v = Cosine of viewing angle

μ_s = Cosine of solar zenith angle

We assume that the atmospheric reflectance due to particle, R_a , is also linear with the τ_a [King, et al., (1999) and Fukushima, et al., (2000)]. This assumption is reasonable because Liu, et al., (1996) also found the linear relationship between both aerosol and molecule scattering.

$$R_a = \frac{\tau_a P_a(\Theta)}{4\mu_s \mu_v} \quad (3)$$

where

τ_a = Aerosol optical thickness (aerosol)

$P_a(\Theta)$ = Aerosol scattering phase function

Atmospheric reflectance is the sum of the particle reflectance and molecule reflectance, R_{atm} , (Vermote, et al., 1997).

$$R_{atm} = R_a + R_r \quad (4)$$

where

R_{atm} = atmospheric reflectance

R_p = particle reflectance

R_r = molecule reflectance

$$R_{atm} = \left[\frac{\tau_a P_a(\Theta)}{4\mu_s \mu_v} + K_1 + \frac{\tau_r P_r(\Theta)}{4\mu_s \mu_v} \right]$$

$$R_{atm} = \frac{1}{4\mu_s \mu_v} [\tau_a P_a(\Theta) + \tau_r P_r(\Theta)] \quad (5)$$

We rewrite the optical depth for particle and molecule as equation (6)

$$\tau = \tau_a + \tau_r \quad (\text{Camagni and Sandroni, 1983}) \quad (6)$$

$$R_{atm} = \frac{1}{4\mu_s \mu_v} [P_a(\Theta) + P_r(\Theta)](\tau) \quad (7)$$

Equations (7) are rewrite into two band equation as equation (8) and (9). The result was extended to a three bands algorithm as equation (11).

$$R_{atm}(\lambda_1) = \frac{1}{4\mu_s \mu_v} [P_a(\Theta, \lambda_1) + P_r(\Theta, \lambda_1)](\tau) \quad (8)$$

$$R_{atm}(\lambda_2) = \frac{1}{4\mu_s \mu_v} [P_a(\Theta, \lambda_2) + P_r(\Theta, \lambda_2)](\tau) \quad (9)$$

$$\tau = a_0 R_{atm}(\lambda_1) + a_1 R_{atm}(\lambda_2) \quad (10)$$

The equation (10) was for two bands, so we rewrite the AOT equation in three bands as

$$\tau = a_0 R_{atm1} + a_1 R_{atm2} + a_2 R_{atm3} \quad (11)$$

where

R_{atmi} = Atmospheric reflectance, $i = 1, 2$ and 3 are the number of the band

e_j = algorithm coefficient, $j = 0, 1, 2$ and 3 are then empirically determined.

4. DATA ANALYSIS AND RESULTS

The satellite Landsat TM7 data used in this study. The surface reflectance was retrieved using ACTOR_2. The reflectance measured from the satellite reflectance at the top of atmospheric, $\rho(\text{TOA})$ was subtracted by the amount given by the surface reflectance to obtain the atmospheric reflectance. And then the atmospheric reflectance was related to the AOT using the regression algorithm analysis. The AOT values were calculated using the Beer-Lambert-Bouguer law from the atmospheric measurements. We selected the spectral wavelength in this study centred at 550 nm. The AOT is related to the transmittance by the expression.

$$T_{d\lambda} = e^{-\frac{\tau_\lambda}{\mu_s}} \quad (\text{Vermote, et al., 1997}) \quad (1)$$

where

$T_{d\lambda}$ = transmittance for direct irradiance at wavelength, λ

μ_s = cosines (θ), θ is the zenith angle

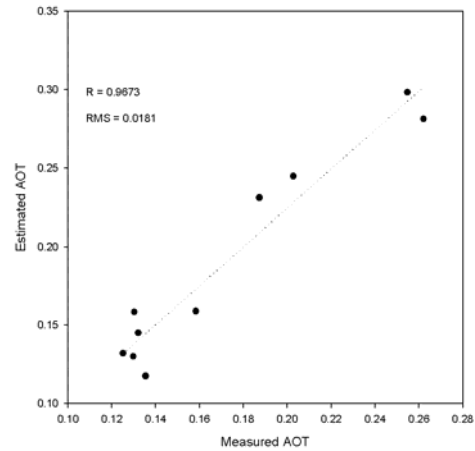


Figure 2. Relationship between measured and estimated AOT

In this study, Landsat TM signals were used as independent variables in our calibration regression analyses. For each regression model the correlation coefficient, R , and

the root-mean-square deviation, RMS, were noted. The proposed algorithm produced higher correlation coefficient between the predicted and the measured AOT values and lower RMS values compared to other algorithms. With the present data set, the R and RMS values were 0.9673 and 0.0181 respectively as indicated in Figure 2.

An AOT map was generated using the proposed algorithm over Mina, Saudi Arabia. And then, the generated AOT map was geometrically corrected using the cubic convolution method to produce a smoother map. The generated map was filtered using 5 by 5 pixels averaged to remove random noise and then colour-coded for visual interpretation as shown in Figure 3.

Figure 3. Map of AOT around Mina, Saudi Arabia (Blue < 0.15, Green = (0.15-0.20), Yellow = (0.20-0.25), Orange = (0.25-0.30), Red = (>0.30) and Black = Water and cloud area)

Algorithm	R	RMS ($\mu\text{g}/\text{m}^3$)
$\text{PM}_{10} = a_0 + a_1 B_1 + a_2 B_1^2$	0.8254	0.0198
$\text{PM}_{10} = a_0 + a_1 B_2 + a_2 B_2^2$	0.5512	0.0215
$\text{PM}_{10} = a_0 + a_1 B_3 + a_2 B_3^2$	0.9025	0.0192
$\text{PM}_{10} = a_0 + a_1 \ln B_1 + a_2 (\ln B_1)^2$	0.8256	0.0199
$\text{PM}_{10} = a_0 + a_1 \ln B_2 + a_2 (\ln B_2)^2$	0.5589	0.0204
$\text{PM}_{10} = a_0 + a_1 \ln B_3 + a_2 (\ln B_3)^2$	0.9256	0.0185
$\text{PM}_{10} = a_0 + a_1 (B_1/B_3) + a_2 (B_1/B_3)^2$	0.6951	0.0201
$\text{PM}_{10} = a_0 + a_1 (B_1/B_2) + a_2 (B_1/B_2)^2$	0.5125	0.0221
$\text{PM}_{10} = a_0 + a_1 (B_2/B_3) + a_2 (B_2/B_3)^2$	0.1951	0.0298
$\text{PM}_{10} = a_0 + a_1 \ln(B_1/B_3) + a_2 \ln(B_1/B_3)^2$	0.6458	0.0198
$\text{PM}_{10} = a_0 + a_1 \ln(B_1/B_2) + a_2 \ln(B_1/B_2)^2$	0.4256	0.0235
$\text{PM}_{10} = a_0 + a_1 \ln(B_2/B_3) + a_2 \ln(B_2/B_3)^2$	0.2584	0.0265
$\text{PM}_{10} = a_0 + a_1 (B_1 - B_2)/B_3 + a_2 ((B_1 - B_2)/B_3)^2$	0.4025	0.0252
$\text{PM}_{10} = a_0 + a_1 (B_1 - B_3)/B_2 + a_2 ((B_1 - B_3)/B_2)^2$	0.4365	0.0231
$\text{PM}_{10} = a_0 + a_1 (B_2 - B_3)/B_1 + a_2 ((B_2 - B_3)/B_1)^2$	0.5545	0.0214
$\text{PM}_{10} = a_0 + a_1 (B_1 + B_3)/B_2 + a_2 ((B_1 + B_3)/B_2)^2$	0.5265	0.0204
$\text{PM}_{10} = a_0 + a_1 (B_2 + B_3)/B_1 + a_2 ((B_2 + B_3)/B_1)^2$	0.4365	0.0245
$\text{PM}_{10} = a_0 + a_1 (B_1 + B_2)/B_3 + a_2 ((B_1 + B_2)/B_3)^2$	0.5685	0.0201
$\text{PM}_{10} = a_0 + a_1 (B_2 - B_1) + a_2 (B_2 - B_1)^2$	0.3912	0.0224
$\text{PM}_{10} = a_0 + a_1 (B_2 - B_3) + a_2 (B_2 - B_3)^2$	0.6365	0.0235
$\text{PM}_{10} = a_0 + a_1 (B_1 - B_3) + a_2 (B_1 - B_3)^2$	0.4025	0.0251
$\text{PM}_{10} = a_0 + a_1 B_1 + a_2 B_2 + a_3 B_3$	0.9673	0.0181

*** B_1 , B_2 and B_3 are the reflectance values for red, green and blue band respectively.**

Table 2. Regression results using different forms of algorithms for AOT.

5. CONCLUSION

In this study, we described the results of AOT mapping using Landsat TM images. The in-situ AOT measurements were derived from atmospheric transmittance measurements using a handheld spectroradiometer. A high correlation was found between the retrieved AOT values and the atmosphere reflectance values. This study indicates that Landsat TM images can be used to provide high accuracy AOT maps.

6. ACKNOWLEDGEMENTS

This project was carried out using the USM research graduate fund and Saudi Arabia government support. We would like to thank the technical staff that participated in this project. Thanks are extended to Universiti Sains Malaysia and Al-Qassim University for support and encouragement.

7. REFERENCES

- Prospero, J. Long-term measurements of the transport of African minerals dust to the southeastern United States: implications for regional air quality, *J.Geophys.Res.*, pp. 15,917–15,927, 1999.
- Wang, J., Nair, U. S. and Christopher, Sundar A. Assimilation of Satellite-derived Aerosol Optical Thickness and Online Integration of Aerosol Radiative Effects in a Mesoscale Model, 13th Conference on Satellite Meteorology and Oceanography, P3.10.
- Camagni, P. and Sandroni, S., 1983, Optical Remote sensing of air pollution, Joint Research Centre, Ispra, Italy, Elsevier Science Publishing Company Inc.
- Fukushima, H., Toratani, M., Yamamiya, S. and Mitomi, Y., 2000, Atmospheric correction algorithm for ADEOS/OCTS ocean color data: performance comparison based on ship and buoy measurements. *Adv. Space Res*, Vol. 25, No. 5, 1015-1024.
- King, M. D., Kaufman, Y. J., Tanre, D. dan Nakajima, T., 1999, Remote sensing of tropospheric aerosol from space: past, present and future, *Bulletin of the American Meteorological Society*, 2229-2259.
- Liu, C. H., Chen, A. J. and Liu, G. R., 1996, An image-based retrieval algorithm of aerosol characteristics and surface reflectance for satellite images, *International Journal of Remote Sensing*, 17 (17), 3477-3500.
- Takemura, T., Nakajima, T., Dubovik, O., Holben, B. N. And Kinne, S., 2002, Single scattering Albedo and radiative forcing of various aerosol species with a global three dimension model, *Journal of Climate*, V 15 (4), 333 – 352.

Vermote, E., Tanre, D., Deuze, J. L., Herman, M. and Morcrette, J. J., 1997, Second Simulation of the satellite signal in the solar spectrum (6S), [Online] available: http://www.geog.tamu.edu/klein/geog661/handouts/6s/6smanv2.0_P1.pdf.